Evaluation of MARC for the Analysis of Rotating Composite Blades

Karen F. Bartos and Michael A. Ernst

NASA

NASA Technical Memorandum 4423

Evaluation of MARC for the Analysis of Rotating Composite Blades

Karen F. Bartos and Michael A. Ernst
Lewis Research Center
Cleveland, Ohio

Summary

The suitability of the MARC code for the analysis of rotating composite blades was evaluated using a four-task process. A nonlinear displacement analysis and subsequent eigenvalue analysis were performed on a rotating spring-mass system to ensure that displacement-dependent centrifugal forces were accounted for in the eigenvalue analysis. Normal modes analyses were conducted on isotropic plates with various degrees of twist to evaluate MARC's ability to handle blade twist. Normal modes analyses were conducted on flat composite plates to validate the newly developed coupled COBSTRAN-MARC methodology. Finally, normal modes analyses were conducted on four composite propfan blades that were designed, analyzed, and fabricated at NASA Lewis Research Center. Results were compared with experimental data. The research documented herein presents MARC as a viable tool for the analysis of rotating composite blades.

Introduction

Since the advent of the Advanced Turboprop Project (ATP), NASA Lewis Research Center has become the lead center in the design and analysis of rotating composite propfan blades (ref. 1). During the ATP program, the Lewis research community expended considerable effort developing the methodologies currently used to structurally analyze composite propfan blades. These methodologies can be, or have been, applied to other rotating components, such as compressor blades and turbine blades. As a result of this effort, the COBSTRAN (COmposite Blade STRuctural ANalyzer) preprocessor code was developed for the generation of composite blade finite element models (ref 2). Given blade geometry and material selection, the COBSTRAN preprocessor combines composite micromechanics and classical laminate theory with a data base of fiber and matrix properties to generate a finite element model with anisotropic material properties. The COBSTRAN code, coupled with MSC or COSMIC NASTRAN, has been the primary tool used thus far for the analysis of these blades.

Recently, the COBSTRAN code was combined with the MARC finite element program. The MARC finite element package is formulated principally for nonlinear analyses (ref. 3). By providing an alternative to NASTRAN, the coupling of MARC with COBSTRAN has the potential to provide the analyst with greater versatility.

This report documents the research done to evaluate the suitability of MARC in the analysis of rotating composite blades. The evaluation process consisted of four tasks. First, a nonlinear displacement analysis and subsequent eigenvalue analysis were performed on a simple spring-mass system subjected to a centrifugal load. This was done to ensure that displacement-dependent centrifugal forces are included in the stiffness matrix used during an eigenvalue analysis. Second, normal modes analyses were conducted on isotropic plates with various degrees of twist, and the results compared with experimental data, to evaluate MARC's ability to handle blade twist. Third, normal modes analyses were conducted on flat composite plates, and the results compared with experimental data. The coupled COBSTRAN-MARC methodology that was developed in this effort was thus validated. Finally, as a direct application of the methodology, normal modes analyses were conducted on four composite propfan blades that were designed, analyzed, and fabricated at NASA Lewis Research Center. Results were compared with holographic data obtained from bench tests conducted on these blades.

Symbols

a	plate length
b	plate width
D	plate flexural rigidity
E	modulus of elasticity
G	shear modulus
h	plate thickness
I	mass moment of inertia
K	spring stiffness
L	Lagrangian function
m	mass
r	initial spring length
V	potential energy
γ	shear strain

ε   direct strain

κ   kinetic energy

λ   frequency parameter

μ   radial displacement

ν   Poisson's ratio

ρ   mass density

σ   direct stress

τ   shear stress

φ   twist angle (root to tip)

Ω   rotational velocity

ω   frequency

Subscripts:

x longitudinal

y transverse

z normal

Centrifugal Softening in Eigenvalue Analysis

When conducting a modal analysis on a rotating, flexible structure, two types of forces are considered: forces due to the component of the centrifugal load that is displacement depen-

Parameter definition section

```
TITLE
TITLE
SIZING,400000,
ELEMENTS,75,
DYNAMIC,2,1,
LARGE DISP
FOLLOW FOR
UPDATE
ALL POINTS
END
```

— Initiates eigenvalue analysis

— Initiates nonlinear displacement analysis

Model definition section

```
.
.
.
.......... MARC MODEL
.
.
ROTATION A
1.,0.,0.,
0.,0.,0.,
DIST LOADS

100,100.,
1,
CONTROL
12,30,

END OPTION
```

— Defines rotational axis

— Applies centrifugal load

History definition section

```
PRINT NODE

MODE,TOTA
2
DIST LOADS

100,0.,
1,
CONTINUE
DIST LOADS

100,0.,
1,
CONTINUE
MODAL SHAPE

CONTINUE
```

— Updates stiffness matrix

Figure 1. — Sample MARC input deck.

dent and forces due to gyroscopic (or Coriolis) effects. These forces are not always accounted for in the respective solution sequences of available finite element packages. With regard to the dynamic analysis of rotating propfan blades, gyroscopic effects are considered negligible because the angular velocity is generally lower than the first modal frequency of the structure (refs. 4 and 5). However, forces due to the component of centrifugal force that is displacement dependent are very important (ref. 6).

The initial step in evaluating MARC's suitability for analyzing rotating, flexible blades was to execute a nonlinear displacement analysis and a subsequent eigenvalue analysis on a rotating spring-mass system. This simple test was used to determine if the component of centrifugal force, dependent upon the translational degrees of freedom lying in the plane of rotation, was accounted for in the stiffness matrix during the eigenvalue analysis. The terms in the stiffness matrix that account for these displacement-dependent centrifugal loads are referred to as "centrifugal-softening" terms.

Centrifugal loads are displacement dependent. As a result, to dynamically analyze a finite element model of a flexible structure experiencing centrifugal loading, a nonlinear displacement analysis is initially required. The nonlinear problem is solved by a series of linear analyses which update load and stiffness matrices. Subsequent to the nonlinear displacement analysis, a modal analysis is performed with the updated mass and stiffness matrices that result from the nonlinear displacement analysis.

By modeling a simple spring-mass system in the plane of rotation, MARC displacement and frequency results at speed were easily compared with the displacement and frequency results obtained from the equation of motion derived in appendix A. For example, when the following nondimensional values are assumed: spring stiffness K of 500, initial spring length v of 1, end mass m of 1, and rotational velocity Ω of 10 rad/sec, the differential equation of appendix A will yield a steady state displacement of 0.25 and a frequency of 20 rad/sec. MARC's nonlinear analysis should converge upon these values. If the stiffness matrix does not account for the centrifugal-softening terms, a frequency of 22.36 rad/sec will result.

Modeling a simple spring-mass system with MARC is not straightforward. There is no provision for defining a point mass at the end of a spring. To resolve this problem, the end mass was modeled with a MARC finite element of extremely small proportions such that the centroid of the element was infinitesimally close to the end node of the spring. The model then consisted of a spring defined between two nodes: one node constrained in all degrees of freedom, and the other coupled to the small finite element representing the end mass. The finite element geometry and material density were defined so that the mass of the element was equal to 1.

Figure 1 shows the MARC input deck required to run nonlinear displacement analysis and subsequent eigenvalue analysis. The MARC input deck is divided into three sections: the parameter definition section, the model definition section,

and the history definition section (ref. 7). In the parameter definition section, the DYNAMIC card flags the eigenvalue analysis, whereas the nonlinear displacement analysis is flagged by the FOLLOW FOR and LARGE DISP cards (ref. 8). The model definition section includes all geometry and material property data, boundary conditions, and initial loading conditions. In particular, the centrifugal force is applied to the model by specifying an IBODY load type of 100 (ref. 9), along with the rotational velocity squared, within the DIST LOAD card block (ref. 8). The rotational axis is specified with the ROTATION A card block (ref. 8). The history definition section controls the loading throughout the subsequent increments of the analysis. The DIST LOAD card blocks included in this section are used only to update the stiffness matrix before an eigenvalue analysis is conducted; therefore, rotational velocity squared is not specified on these cards.

The element library of the MARC code contains over 100 different element formulations. Only shell elements were chosen for evaluation. Among the available shell elements, 7 elements looked practical for rotating blade applications: elements 3, 22, 26, 49, 50, 72, and 75 (ref. 9). The end mass of the spring-mass system was modeled with each of these elements in turn. Analyses conducted with elements 3, 22, 26, and 75 were found to correctly solve for the displacement and eigenvalue of the spring-mass problem previously discussed. Appendix B summarizes the formulations for these elements. Table I gives the results of analyses using these four elements. It is not understood why the remainder of the shell elements tested did not correctly solve the spring-mass problem.

When modeling a rotating, flexible structure with element 3, 22, 26 or 75, MARC will correctly perform a nonlinear displacement analysis and subsequent eigenvalue analysis without special programming to update the stiffness matrix with centrifugal-softening terms. Because of the two-dimensional nature of elements 3 and 26, the remainder of this study was restricted to elements 22 and 75.

TABLE I.– RESULTS FROM ROTATING SPRING-MASS
SYSTEM PROBLEM

MARC element		Displacement	Converged in increment	Eigenvalue
3	☐	0.25129	1	19.9996
3	△	.25089	1	19.9995
22	☐	.25129	2	19.9996
22	△	.25089	2	19.9995
26	☐	.25129	2	19.9996
26	△	.25089	2	19.9995
75	☐	.25129	1	19.9996
75	△	.25089	1	19.9995

3

To demonstrate MARC's ability to properly handle the physics of centrifugal loading during a modal analysis run, a flat plate was modeled and analyzed at rotational velocities of 2000, 4000, and 5000 rpm for plate setting angles of 0° and 90° with respect to the plane of rotation. When the plate is lying in the plane of rotation (0° orientation), the stiffness associated with the translational degrees of freedom perpendicular to the plate does not experience centrifugal softening; however, when the plate is perpendicular to the plane of rotation (90° orientation), the stiffness associated with the same degrees of freedom does experience centrifugal softening. Therefore, it was expected that the first bending frequency of the flat plate lying in the plane of rotation would be higher at rpm than the first bending frequency of the flat plate perpendicular to the plane of rotation.

The flat plate modeled was 7 in. long, 3 in. wide, and 1/8 in. thick. The finite element model of the flat plate was composed of 65 quadrilateral elements (because of its simplicity, MARC element type 75 was used). Figure 2 displays the model and lists the material properties used. All six nodal degrees of freedom were constrained along the short edge of the plate closest to the axis of rotation. The axis of rotation was 7 in. from the constrained edge of the plate.

Figure 3 shows the first bending frequencies of the flat plate at rpm for the two plate orientations of 0° and 90°. As expected, at rpm the first bending frequency of the flat plate lying in the plane of rotation was higher than that for the flat plate perpendicular to the plane of rotation. Identical results were obtained by analyzing an equivalent finite element model subjected to the same boundary conditions with MSC/NASTRAN using extensive DMAP programming (ref. 6). With MARC, however, no special programming was required to add centrifugal-softening terms into the global stiffness matrix utilized by the modal analysis.

Note that several of the MARC element types (elements 50 and 72) that failed the rotating spring-mass problem were again tested in this flat plate analysis. The frequencies were identical to those shown in figure 3. Erroneous results with centrifugal loading problems occurred when the finite element model was constrained with springs. Because situations may arise when spring elements are used to simulate the hub stiffness associated with a particular rotating blade (ref. 10), it is recommended that finite element models of rotating structures be created only with the plate elements that properly solved the rotating spring-mass problem discussed here.

Isotropic Twisted Plate Study

Blade twist is one geometric aspect of rotating blades that concerns the analyst. When modeling twisted blades with quadrilateral elements, element nodes generally are not coplanar. For certain finite elements, this may result in an additional stiffness that is inaccurate (ref. 11). Reference 12 presents

Properties
Modulus of elasticity = 15.5x10⁶ psi
Shear modulus = 6.5x10⁶ psi
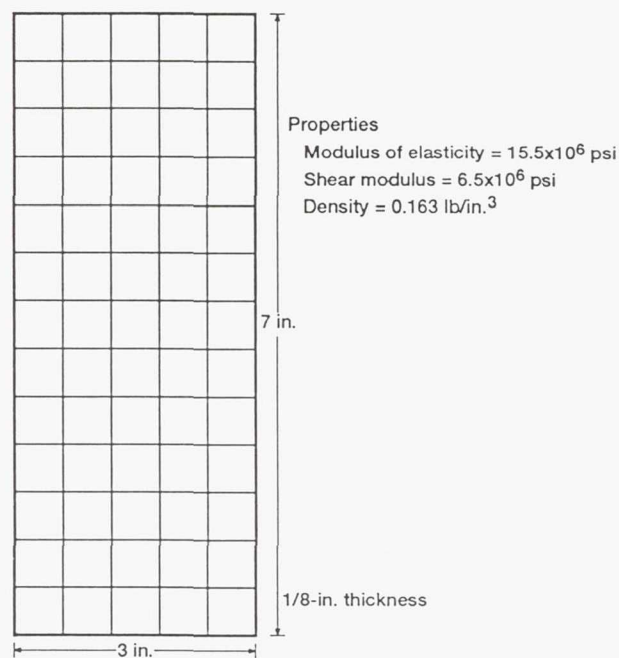Density = 0.163 lb/in.³

7 in.

1/8-in. thickness

3 in.

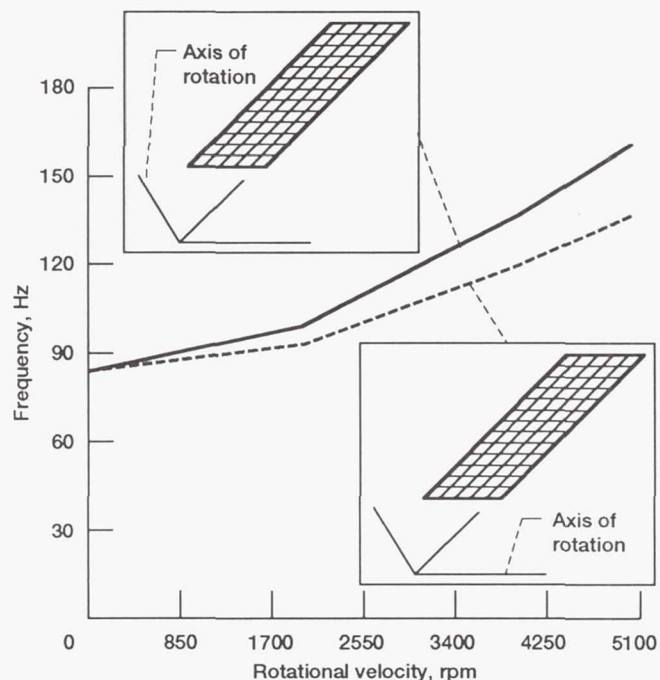Figure 2. — Finite element model of flat plate.

Figure 3. — Effect of centrifugal softening on first bending frequencies of flat plate.

experimental frequencies for various cantilevered isotropic twisted plates of uniform thickness. A normal modes analysis was conducted on a selected number of twisted plates and compared with the experimental results found in reference 12. This was done to assess MARC's ability to perform such analyses when blades are modeled with element 75 or 22.

Reference 12 presents experimental frequencies and mode shapes for various cantilevered twisted plates machined out of 7075–T6 cold-drawn aluminum bar stock (fig. 4). Reference 13 provides detailed information on the experimental methods used. Twenty twisted plates, consisting of all combinations of two aspect ratios ($a/b = 1$ and 3), two thickness ratios ($b/h = 5$ and 20), and five twist angles ($\phi = 0°, 15°, 30°, 45°,$ and $60°$) were machined. All the plates had a rectangular cross section with a width b of 2 in. Frequencies documented in reference 12 were reported in the form of the standard plate nondimensional frequency parameter:

$$\lambda = \omega \times a^2 \times \sqrt{\frac{\rho \times h}{D}}$$

where D is the plate flexural rigidity,

$$D = \frac{E \times h^3}{12 \times (1 - v^2)}$$

This study was restricted to plates with thickness ratios of 20 and aspect ratios of 3 because these plates reflect the geometric traits of most propfan blades. Two sets of finite element models were generated for plates with twist angles of $0°, 30°,$ and $60°$ (fig. 5): one set comprising 384 4-noded quadrilateral elements (MARC element 75), and one set comprising 60 8-noded quadrilateral elements (MARC element 22). For each model, nodal degrees of freedom were fully constrained along one of the short edges. A modulus of elasticity E of 10.3×10^6 psi, Poisson's ratio v of 0.33, and mass density ρ of 0.101 lb/in.^{2} were assumed.

A MARC normal modes analysis was conducted on each of the models generated. Analytical mode shapes and frequencies were recorded for the first three bending modes, the first two torsional modes, and the first edgewise mode. All frequencies were put in the form of the standard plate nondimensional frequency parameter λ. Results from the analyses are presented in figures 6 and 7 for the models consisting of elements 75 and 22, respectively. Table II presents a comparison between analytical and experimental nondimensional frequencies. An experimental first edgewise frequency is not available for the plate with 0° twist. Generally, analytical frequencies correlated very well with experimental frequencies. However, poor correlation was noted for the 3rd bending mode associated with the plate with 30° twist, and for all edgewise modes.

Flat Composite Plate Analysis

Composite materials are being used more frequently in the construction of rotating blades. However, few finite element codes provide composite analysis capability that reflects actual composite blade construction. As mentioned in the introduction, the COBSTRAN preprocessor code was developed for the generation of composite blade finite element models (refs. 2 and 14). Formerly, COBSTRAN generated either MSC or COSMIC NASTRAN input decks. The COBSTRAN code has recently been modified so that a MARC input deck for a blade model can also be created. At this time, only a model using MARC element 75 is output by COBSTRAN. In order to verify the modified version of COBSTRAN, as well as MARC's ability to analyze composite blades, a normal modes analysis was performed on flat composite plates that were previously dynamically bench tested. MARC eigenvalues were compared with those generated by MSC/NASTRAN and the dynamic bench test. Three flat graphite-epoxy composite plates, designated form 1, form 2, and form 3, were modeled and analyzed. Figure 8 shows the finite element model, material properties, geometry, and ply lay-up for the three plates. Each plate was made of 18 plies resulting in a thickness of 0.09 in. The composite plies were symmetrical about the midplane of the plates and were stacked from the surface to the point of midthickness. All plies were oriented with respect to the spanwise axis (from base to tip). Starting with the outside ply and working toward the point of midthickness, the plates were fabricated with the ply groups shown in figure 8. Finite element models of these flat plates were generated with COBSTRAN and analyzed with both MARC and MSC/NASTRAN. Quadrilateral elements were used because, at this time, the COBSTRAN code does not provide for the output of a MARC model that has triangular elements. The model was constrained in all degrees of freedom at the eight nodes along the base of the plate.

The experimental data used for comparison with the analytical results were obtained from a pending reference publication (T.J. Sutliff et al., to be published). In this investigation, vibration mode frequency and shape evaluations were made on three cantilevered composite plate specimens described in figure 8.
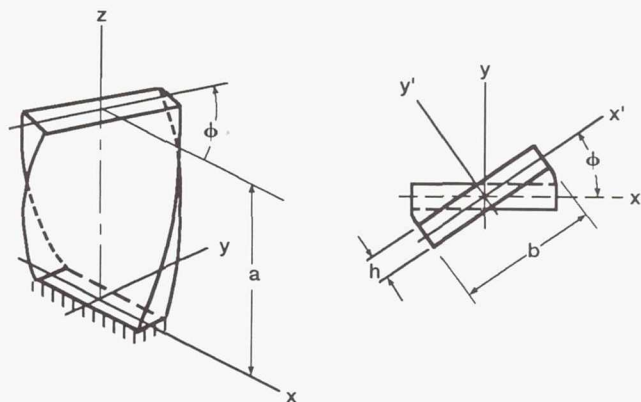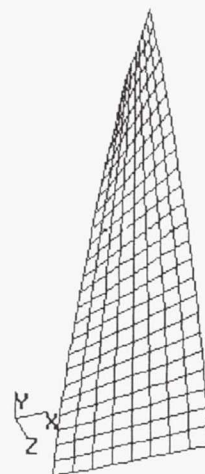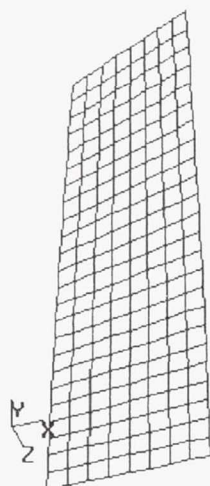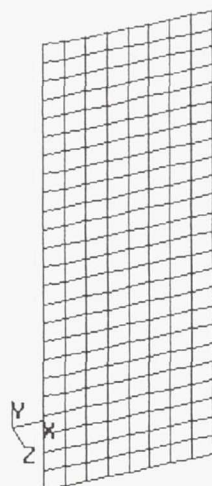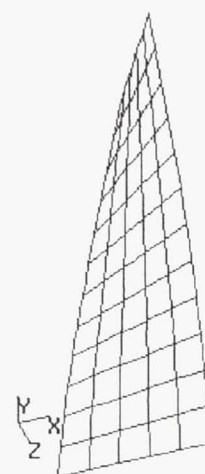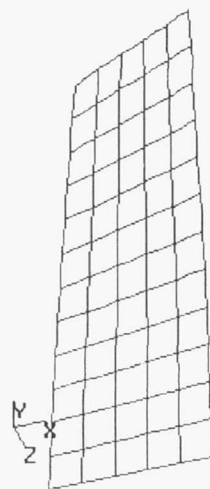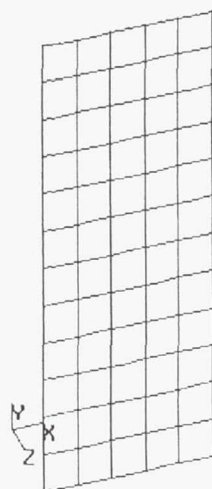

Figure 4. — Twisted cantilevered plate.

Element 75

Element 22

0° Twist   30° Twist   60° Twist

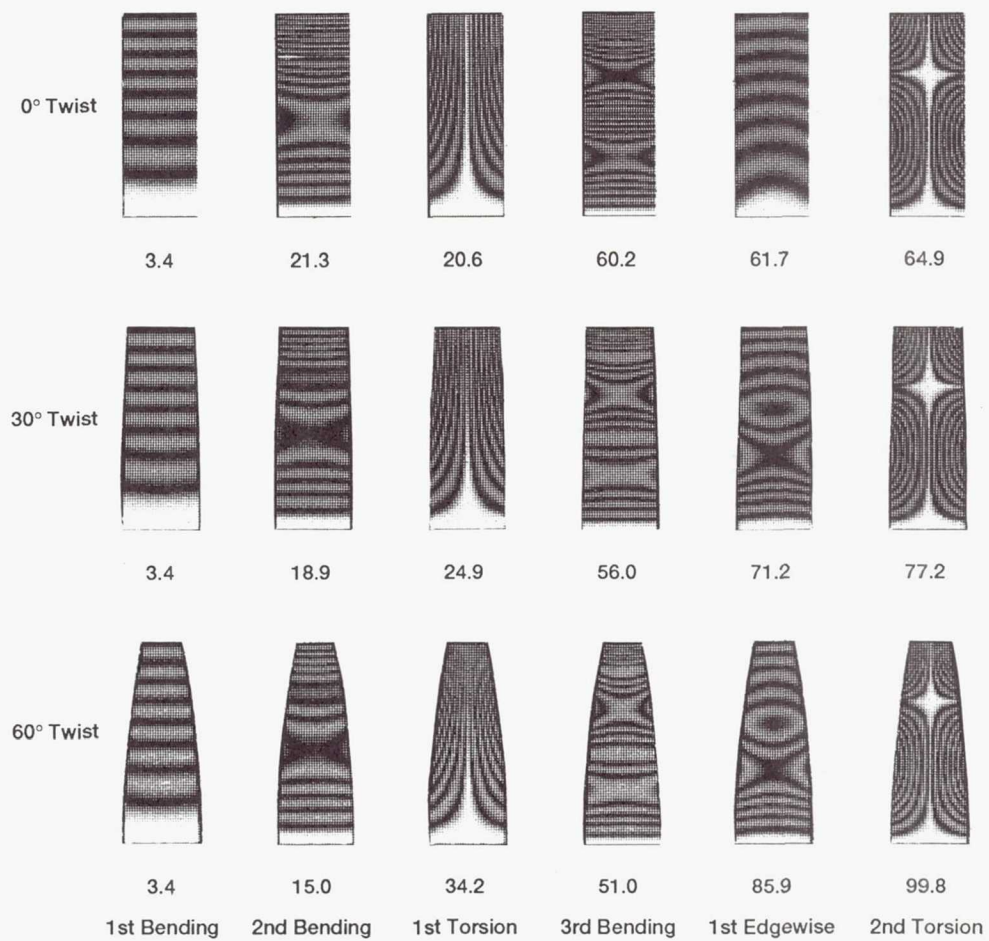Figure 5. — Twisted plate study; MARC finite element models.

3.4	21.3	20.6	60.2	61.7	64.9

0° Twist

30° Twist

3.4	18.9	24.9	56.0	71.2	77.2

60° Twist

3.4	15.0	34.2	51.0	85.9	99.8
1st Bending	2nd Bending	1st Torsion	3rd Bending	1st Edgewise	2nd Torsion

Figure 6. — Twisted plate study; MARC element 75 results. (Nondimensional frequencies are presented.)

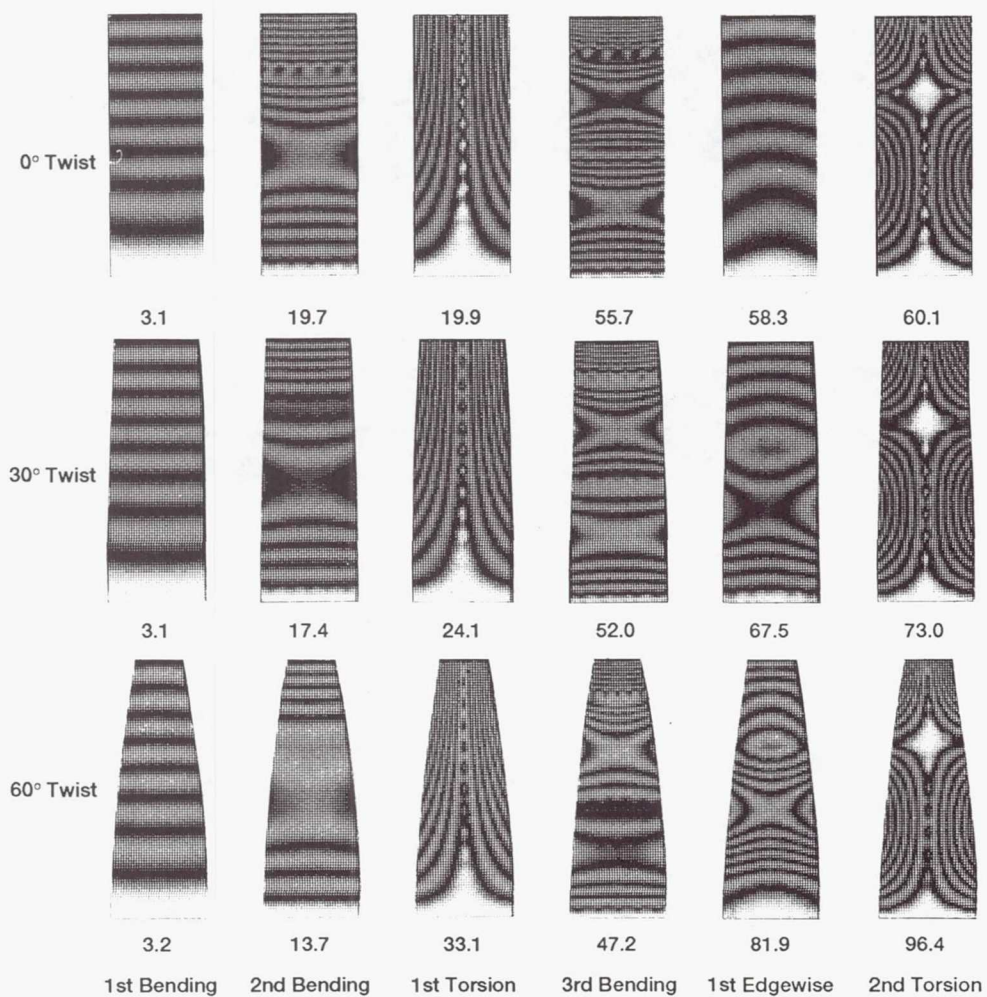|					
0° Twist					
3.1	19.7	19.9	55.7	58.3	60.1
30° Twist					
3.1	17.4	24.1	52.0	67.5	73.0
60° Twist					
3.2	13.7	33.1	47.2	81.9	96.4
1st Bending	2nd Bending	1st Torsion	3rd Bending	1st Edgewise	2nd Torsion

Figure 7. — Twisted plate study; MARC element 22 results. (Nondimensional frequencies are presented.)

TABLE II. – TWISTED PLATE STUDY

Mode	Experiment	MARC element 75 QUAD–4	Difference from experiment, %	MARC element 22 QUAD–8	Difference from experiment, %
Twist angle, 0°					
1st Bending	3.32	3.40	2.41	3.14	−5.42
2nd Bending	20.76	21.30	2.60	19.70	−5.11
1st Torsion	19.58	20.61	5.26	19.93	1.79
3rd Bending	58.65	60.20	2.64	55.71	−5.01
2nd Torsion	62.43	64.90	3.96	60.08	−3.76
1st Edgewise	N/A	61.70	N/A	58.34	N/A
		Average	3.37	Average	−3.50
Twist angle, 30°					
1st Bending	3.28	3.40	3.66	3.14	−4.27
2nd Bending	18.03	18.94	5.05	17.45	−3.22
1st Torsion	23.53	24.90	5.82	24.08	2.34
3rd Bending	46.29	56.01	21.00	52.02	12.38
2nd Torsion	71.61	77.25	7.88	72.97	1.90
1st Edgewise	57.98	71.22	22.84	67.50	16.42
		Average	11.04	Average	4.26
Twist angle, 60°					
1st Bending	3.22	3.40	5.59	3.15	−2.17
2nd Bending	14.09	15.03	6.67	13.74	−2.48
1st Torsion	32.29	34.18	5.85	33.12	2.57
3rd Bending	47.68	51.02	7.01	47.22	−0.96
2nd Torsion	94.02	99.80	6.15	96.43	2.56
1st Edgewise	73.47	85.87	16.88	81.88	11.45
		Average	8.02	Average	1.83

Material
  Fiberite 2148A1A epoxy

Properties
  Fiber volume ratio 0.604
  Weight density, lb/in.^{3} . . . . .0.560x10^{-1}
  Longitudinal modulus, lb/in.^{2} . . . . 0.347x10^8
  Transverse modulus, lb/in.^{2} . . . . 0.110x10^7
  Shear modulus, lb/in.^{2} . . . . 0.800x10^6
  Poisson's ratio 0.300

Composite ply strengths
  Longitudinal tensile, lb/in.^{2} . . . . 0.146x10^6
  Longitudinal compressive, lb/in.^{2} . . . . 0.146x10^6
  Transverse tensile, lb/in.^{2} . . . . 0.150x10^5
  Transverse compressive, lb/in.^{2} . . . . . 0.210x10^5
  Intralaminar shear, lb/in.^{2} . . . . 0.118x10^2

Ply lay-up
  Form 1 (0   0   90   90   0   0   90   90   0)
  Form 2 (0   0   45   90   -45   0   45   0   -45)
  Form 3 (0   45   0   -45   0   45   0   -45   0)
              ↑   ↑

           Plate   Plate
          surface   midthickness

8 in.

0.09-in. thickness

|←———2 in.———→|

Figure 8. — Composite flat plate model, forms 1, 2, and 3.

	91.9 Hz	572.8 Hz	1595.5 Hz	3106.3 Hz
NASTRAN				
MARC	83.9 Hz	524.8 Hz	1465.2 Hz	2860.8 Hz
Test	91.6 Hz	554.3 Hz	1526.3 Hz	2918.0 Hz

Figure 9. — Results for composite plate, form 1.

NASTRAN

| 90.1 Hz | 441.8 Hz | 564.3 Hz | 1409.0 Hz | 1585.1 Hz |

MARC

| 81.8 Hz | 518.7 Hz | 511.4 Hz | 1621.6 Hz | 1432.8 Hz |

Test

| 89.0 Hz | 415.7 Hz | 539.1 Hz | 1318.8 Hz | 1491.8 Hz |
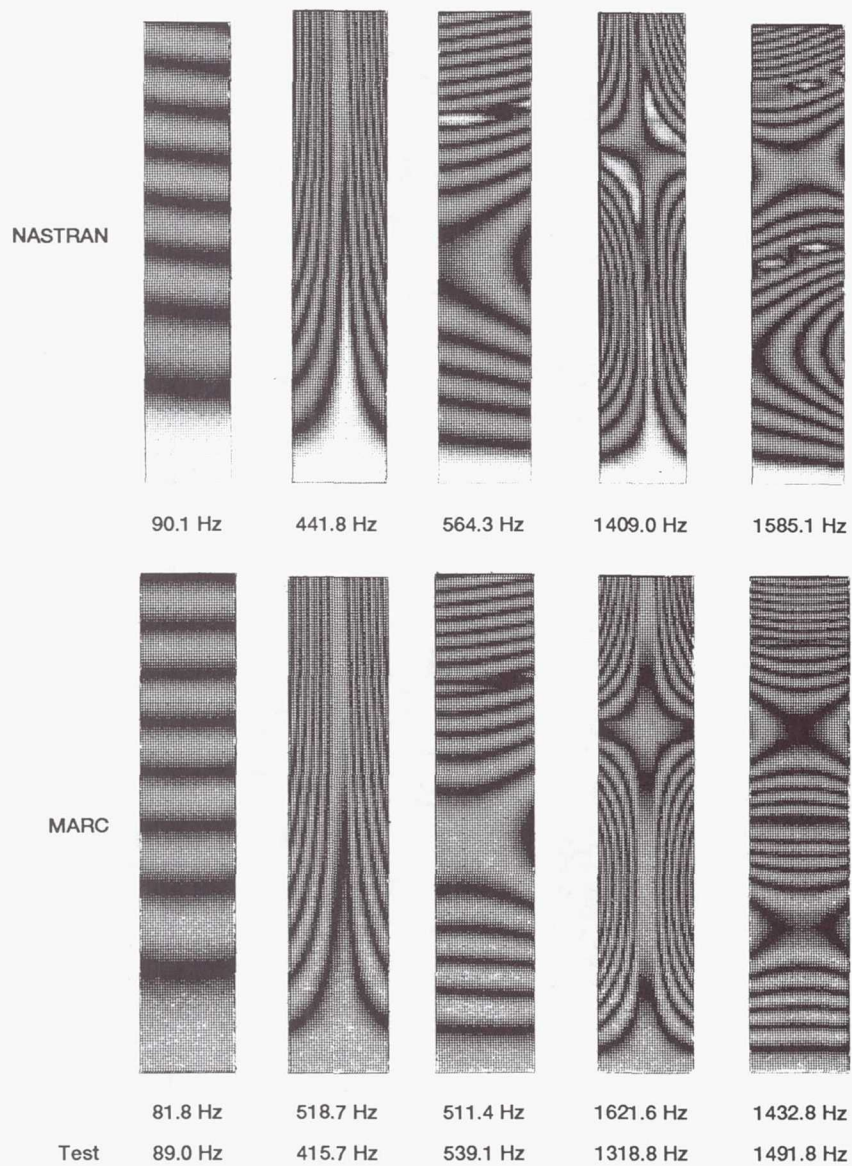
Figure 10. — Results for composite plate, form 2.

NASTRAN

| | | | | Not available | Not available | |

90.1 Hz   496.9 Hz   561.3 Hz   1555.5 Hz   1590.6 Hz

MARC

Not available   Not available

88.4 Hz   523.4 Hz   550.4 Hz   1644.4 Hz   1545.1 Hz

Test   89.2 Hz   466.8 Hz   535.7 Hz   1455.6 Hz   1465.9 Hz   1493.4 Hz
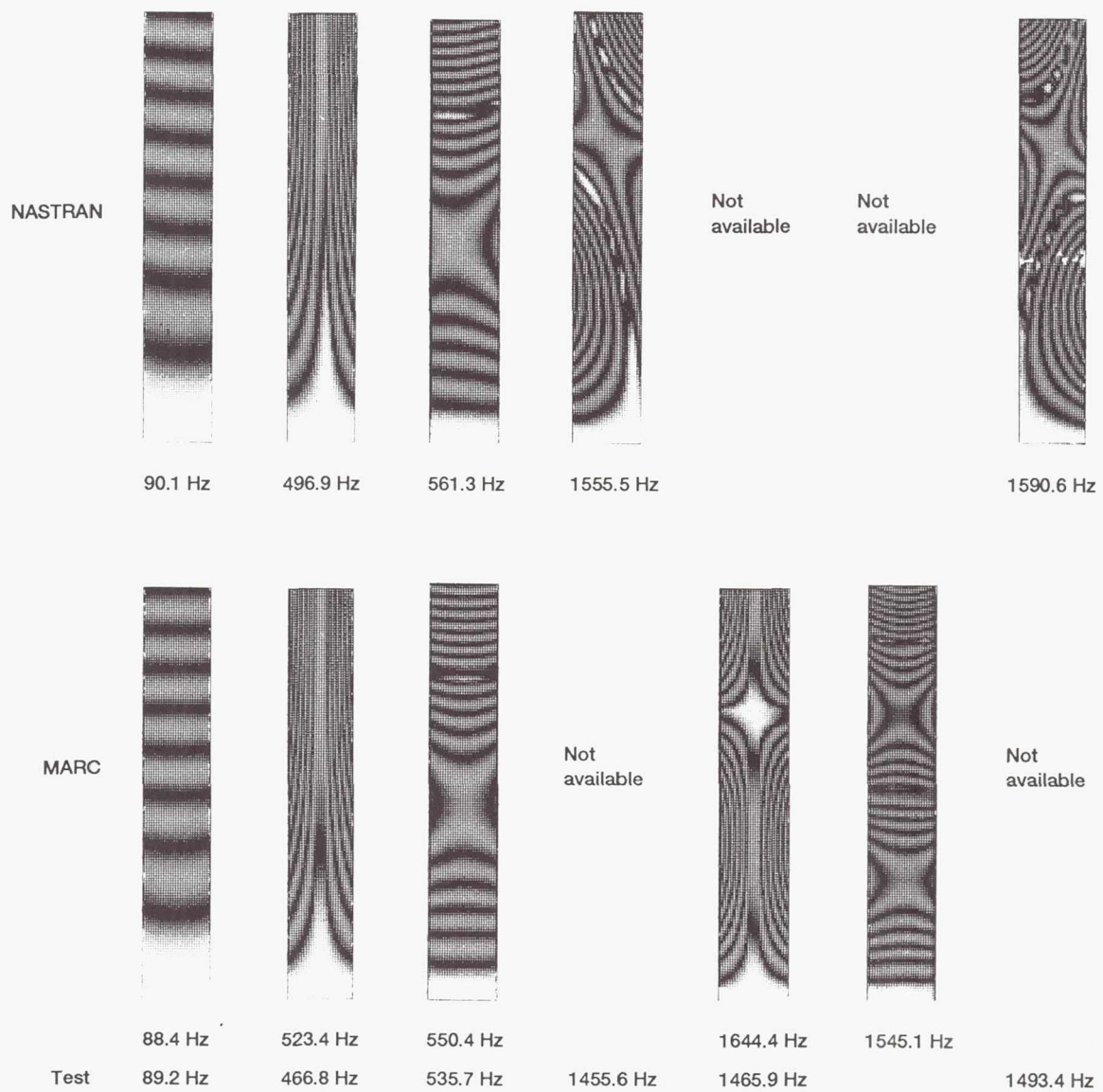
Figure 11. — Results for composite plate, form 3.

TABLE III. – SUMMARY OF COMPOSITE FLAT PLATE ANALYSES

Mode	Experiment	MARC	Difference from experiment, %	NASTRAN	Difference from experiment, %
Form 1					
1st Bending	91.6	83.9	−8.4	91.9	0.3
2nd Bending	554.3	524.8	−5.3	572.8	3.3
3rd Bending	1526.3	1465.2	−4.0	1595.5	4.5
4th Bending	2918.0	2860.8	−2.0	3106.3	6.4
Form 2					
1st Bending	89.0	81.8	−8.1	90.1	1.2
1st Torsion	415.7	518.7	24.8	441.8	6.3
2nd Bending	539.1	511.4	−5.1	564.3	4.7
2nd Torsion	1318.8	1621.6	23.0	1409.0	6.8
3rd Bending	1491.8	1432.8	−4.0	1585.1	6.2
Form 3					
1st Bending	89.2	88.4	−0.9	90.1	1.0
1st Torsion	466.8	523.4	12.1	496.9	6.4
2nd Bending	535.7	550.4	2.7	561.3	4.8
Mix1[a]	1455.6	N/A	N/A	1555.5	6.9
2nd Torsion	1465.9	1644.4	12.2	N/A	N/A
3rd Bending	N/A	1545.1	N/A	N/A	N/A
Mix2[b]	1493.4	N/A	N/A	1590.6	6.5

[a]First coupled bending/torsion.
[b]Second coupled bending/torsion.

Figures 9 to 11 display mode shapes and eigenvalues from the MARC and NASTRAN analyses, along with the corresponding test results, for each of the three forms of the composite plate. Table III presents the tabulated results. From this study, some general observations can be made. First, MARC torsional frequencies are generally higher than NASTRAN or experimental torsional frequencies, whereas MARC bending frequencies are generally lower than NASTRAN or experimental bending frequencies. The second bending mode of form 3 is an exception. Second, MARC eigenvalues correlate better with experimental results when the ply pattern is recurrent throughout the laminate. For example, the composite ply lay-ups for forms 1 and 3 are recurrent, whereas the composite ply lay-up for form 2 is irregular. Third, MARC-generated mode shapes tend to be very symmetrical, whereas NASTRAN-generated mode shapes tend to be unsymmetrical. With regard to the composite plate form 3 analysis (fig. 11), note that certain mode shapes were missed by MARC, and others, by NASTRAN.

Analysis of Composite Propfan Blades

The NASA Lewis Research Center designed, analyzed, and fabricated counter-rotating composite propfan blades for a 0.55-scale cruise missile wind tunnel model (ref. 15). Figure 12 shows a drawing of this cruise missile. Two sets of forward and aft blades were designed and fabricated: one set
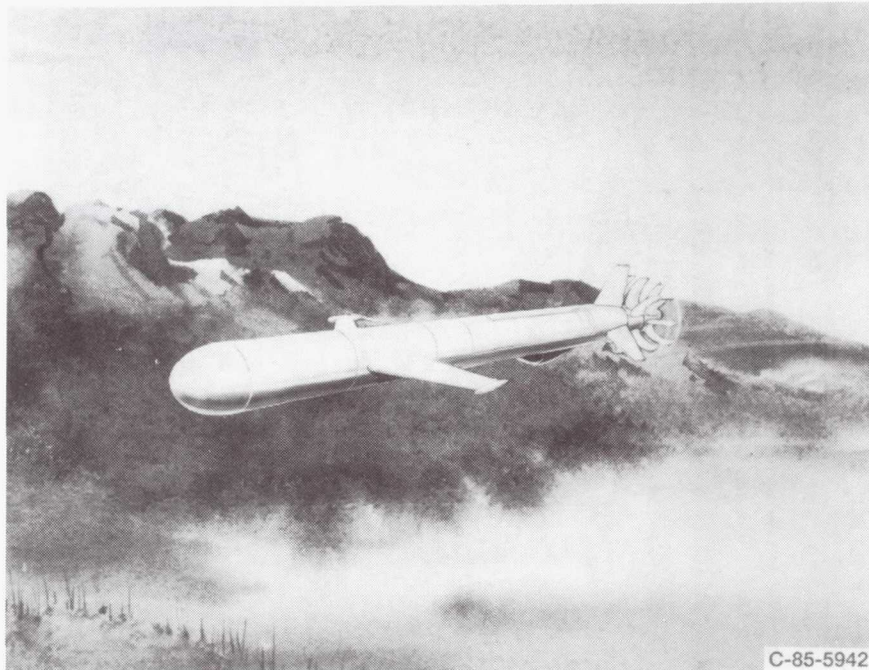
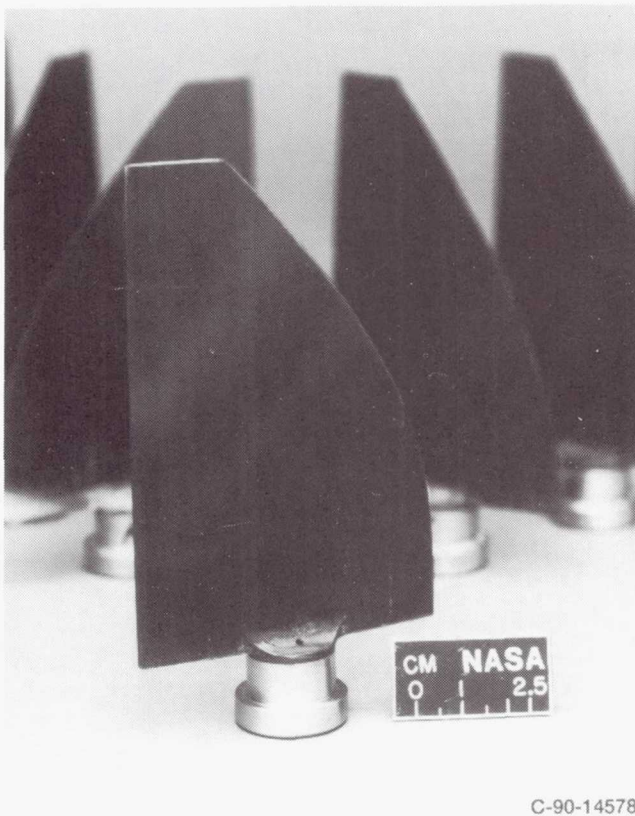Figure 12. — Cruise missile conceptual design.

C-90-14578

Figure 13. — CM1 propfan blade.

is designated the CM1 series (fig. 13), and the other set is designated the CM2 series (fig. 14). Details on the geometric design of these blades can be found in references 16 and 17. Originally, these blades were dynamically analyzed with MSC/NASTRAN's version 65C (refs. 18 and 19). Recently, a normal modes analysis was conducted on these propfan blades with MARC. This study was carried out as the final step in the evaluation of MARC for use in analyzing rotating composite propfan blades. Mode shapes and frequencies resulting from the analyses were compared with those obtained from MSC/NASTRAN and with those obtained from holographic testing (ref. 20).

All four propfan blades were fabricated with graphite-epoxy composite plies. Each ply had a thickness of 0.0032 in. Table IV presents the material properties for these plies. The

TABLE IV. — MATERIAL PROPERTIES FOR
GRAPHITE EPOXY PLIES

Fiber volume ratio	0.604
Weight density, $lb/in.^3$	0.560×10^{-1}
Longitudinal modulus, $lb/in.^2$	0.194×10^8
Transverse modulus, $lb/in.^2$	0.120×10^7
Shear modulus, $lb/in.^2$	0.700×10^6
Poisson's ratio	0.310
Longitudinal tensile strength, $lb/in.^2$	0.266×10^6
Longitudinal compressive strength, $lb/in.^2$	0.266×10^6
Transverse tensile strength, $lb/in.^2$	0.930×10^4
Transverse compressive strength, $lb/in.^2$	0.930×10^4
Intralaminar shear strength, $lb/in.^2$	0.130×10^5

15
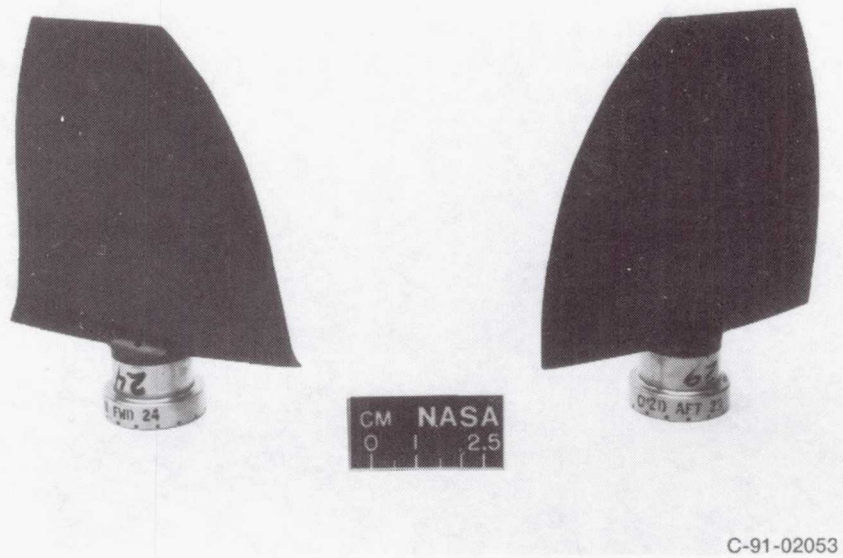
Figure 14. — CM2 propfan blade.
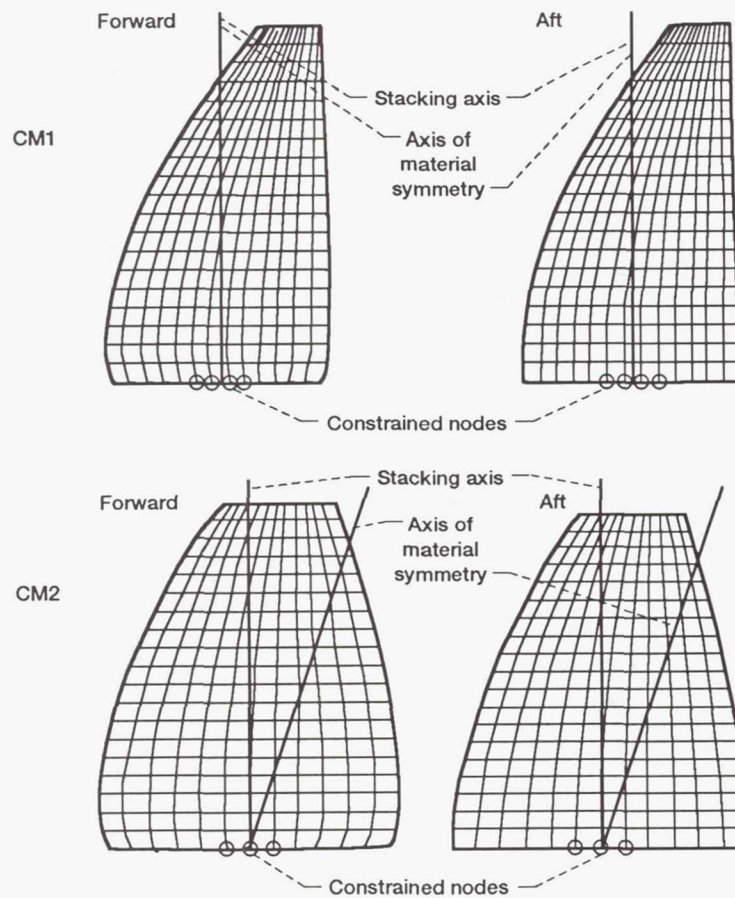
Figure 15. — Composite blade finite element models.

composite plies were symmetrical about the midplane of the blades and were stacked from the surface to the point of mid-thickness. Because the thickness of the blades varies from root to tip and from leading edge to trailing edge, the composite plies were contoured such that ply size diminished when working from the surface to the point of midthickness. All plies were oriented with respect to the spanwise/stacking axis (from base to tip; see fig. 15). Angles were positive when plies were oriented toward the trailing edge of the blades. Starting with the outside ply and working toward the point of midthickness, the CM1 blades were fabricated with a repeating ply group of $[0°, 0°, 45°, 0°, 0°, -45°]$. The CM2 blades were fabricated with a repeating ply group of $[20°, 20°, 65°, 20°, 20°, -25°]$. Reference 21 provides further details on the fabrication of these propfan blades.

All MARC finite element models pertaining to the cruise missle propfan blades were generated with the COBSTRAN preprocessor code and utilized MARC's element 75. When generating MARC finite element models of composite propfan blades, equivalent material properties of the composite lami-nate are specified for each finite element with MARC's ORTHOTROPIC material definition block (ref. 8). The aniso-tropic material properties were defined in a coordinate system whose primary axis lies along the stacking axis shown in figure 15. The material properties were then incorporated into stress-strain laws for the generation of a "compliance" matrix (ref. 7) for elements 22 and 75:

$$
\begin{Bmatrix} \varepsilon_{xx} \\ \varepsilon_{yy} \\ \gamma_{xy} \\ \gamma_{yz} \\ \gamma_{zx} \end{Bmatrix} = \begin{bmatrix} 1/E_{xx} & -v_{yx}/E_{yy} & 0 & 0 & 0 \\ -v_{xy}/E_{xx} & 1/E_{yy} & 0 & 0 & 0 \\ 0 & 0 & 1/G_{xy} & 0 & 0 \\ 0 & 0 & 0 & 1/G_{yz} & 0 \\ 0 & 0 & 0 & 0 & 1/G_{zx} \end{bmatrix}
$$

$$
\times \begin{Bmatrix} \sigma_{xx} \\ \sigma_{yy} \\ \tau_{xy} \\ \tau_{yz} \\ \tau_{zx} \end{Bmatrix}
$$

MARC's compliance matrix is not fully populated because the orthotropic material properties are defined along the material axis of symmetry. Thus, the longitudinal and transverse strains are uncoupled from the shear stresses, and the shear strains are uncoupled from the longitudinal and transverse stresses.

As mentioned earlier, the composite ply lay-up for the CM2 forward and aft blades was a repeating ply group of $[20°, 20°,$

$65°, 20°, 20°, -25°]$ with respect to the stacking axis. Because of the simplistic nature of the ply lay-up, it can be seen that the axis of material symmetry was off by 20° from the stacking axis of the blade. Because COBSTRAN always generates finite element models such that the primary axis of the material coordinate system lies along the "stacking" axis of the blade, and MARC requires properties about the material axis of symmetry, COBSTRAN would not directly generate a MARC finite element model that accurately reflected the CM2 design. This was not a problem with the CM1 design because the axis of material symmetry coincided with the stacking axis.

To remedy the problem, the equivalent laminate material properties for each element of the CM2 blade were redefined within the MARC input deck: specifically, the properties were written in a local material coordinate system where the pri-mary axis coincided with the material axis of symmetry. This was accomplished by using COBSTRAN to regenerate the finite element model with a repeating ply group of $[0°, 0°, 45°, 0°, 0°, -45°]$ with respect to the stacking axis. By adding 20° to the orientation angles defined in the ORIENTATION defi-nition data block (ref. 8), the material coordinate system for each element was redefined such that the primary axis was rotated 20° from the stacking axis about the local element normal. The COBSTRAN-generated MARC model then accurately reflected the CM2 blade design.

A normal modes analysis was conducted on all four propfan blade models using MARC. MARC finite element models of the CM1 forward and aft blades comprised 247 quadrilateral elements. In all, the elements were defined by 280 coordi-nates: 14 coordinates for each of 20 spanwise stations of the blade. CM2 forward and aft models comprised 228 quadrilat-eral elements. The elements in the CM2 models were defined by 260 nodes: 13 coordinates for each of 20 spanwise stations. Translational and rotational degrees of freedom of nodes closely approximating the location of the blade-to-hub inter-face were fully constrained: four nodes at the base of the CM1 models, located about the midchord, were fully constrained; while three nodes at the base of the CM2 models were fully constrained. For comparison, the finite element models docu-mented in references 18 and 19 were reinvestigated with MSC/NASTRAN's normal modes analysis using the same boundary conditions imposed upon the MARC models shown in figure 15. The only difference between the MARC and NASTRAN models was the type of elements used: triangular elements were used in the NASTRAN models, whereas quad-rilateral elements were used in the MARC models.

Figures 16 to 19 show the resulting mode shapes and frequencies obtained from these analyses. MARC and NASTRAN mode shapes and frequencies correlated well with experimental results. With the exception of the first bending frequencies for the CM2 forward and aft blades, MARC analytical frequencies were lower than NASTRAN analytical frequencies.
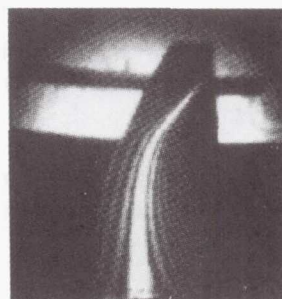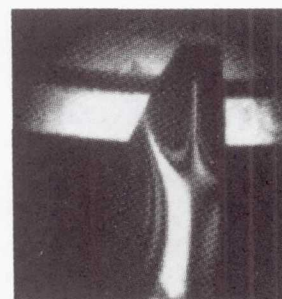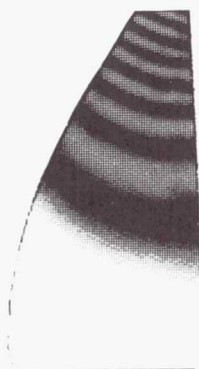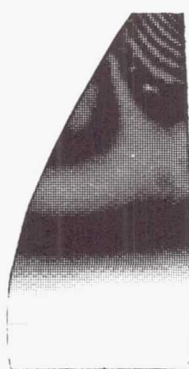
Experimental
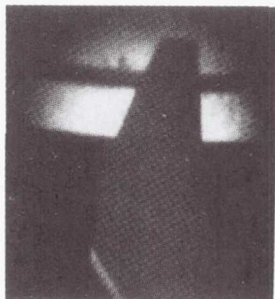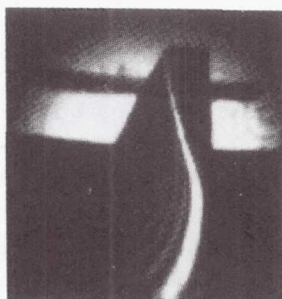
831 Hz   1798 Hz   2107 Hz   2673 Hz
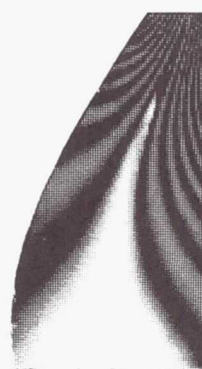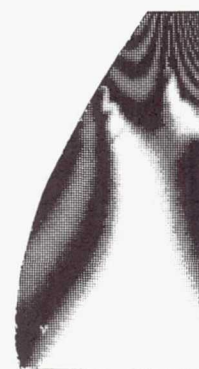
NASTRAN

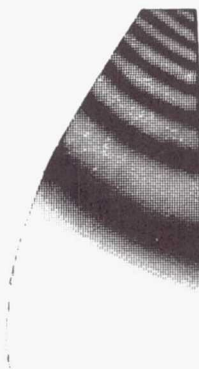944.6 Hz   2112.0 Hz   2371.3 Hz   3161.5 Hz
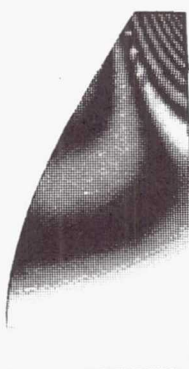
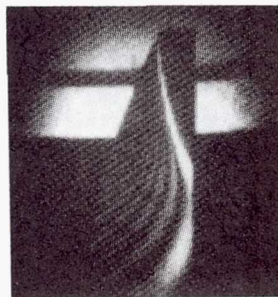MARC

922.0 Hz   1962.9 Hz   2278.1 Hz   2881.5 Hz

Figure 16. — Results for CM1 forward blade.

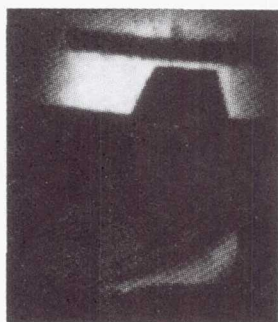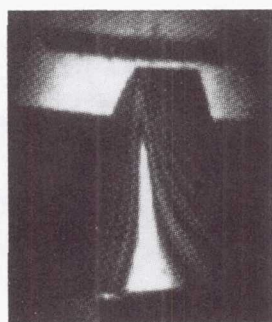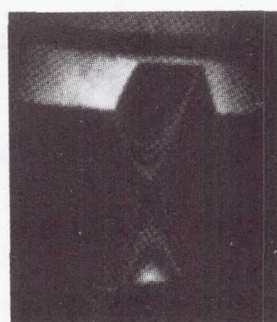|			
Experimental	833 Hz	1731 Hz	2131 Hz	2570 Hz
NASTRAN	922.6 Hz	2021.6 Hz	2365.3 Hz	3083.4 Hz
MARC	921.9 Hz	1924.0 Hz	2302.8 Hz	2846.3 Hz
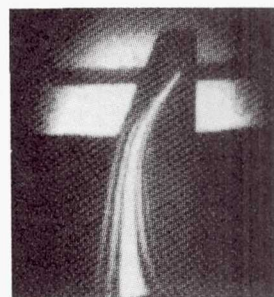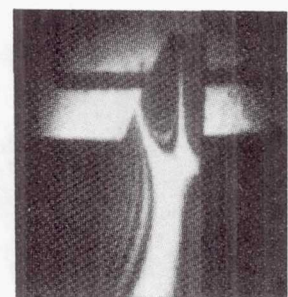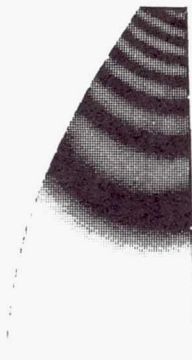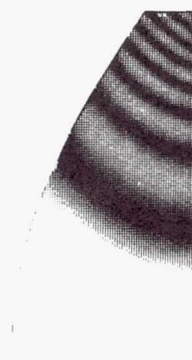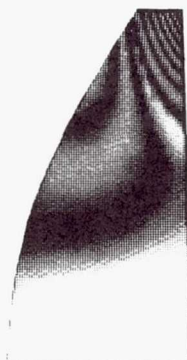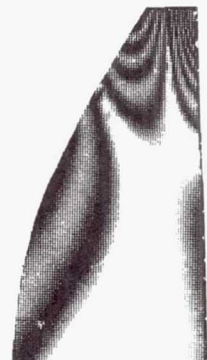
Figure 17. — Results for CM1 aft blade.
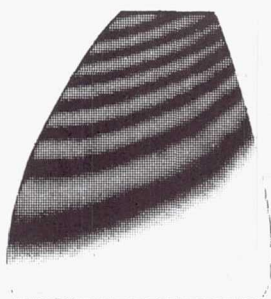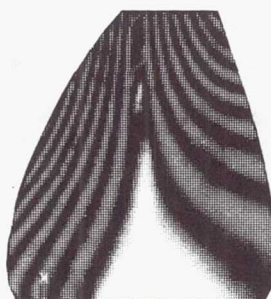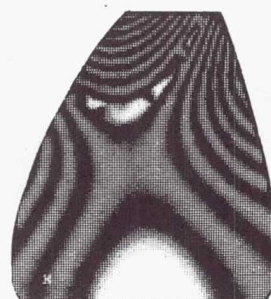
Experimental

| 956 Hz | 1677 Hz | 2416 Hz | 3226 Hz |

NASTRAN

| 980.4 Hz | 1884.4 Hz | 2602.8 Hz | 3510.3 Hz |
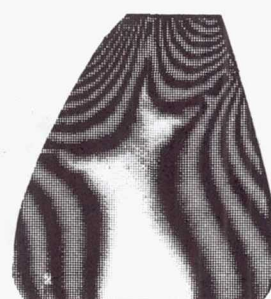
MARC
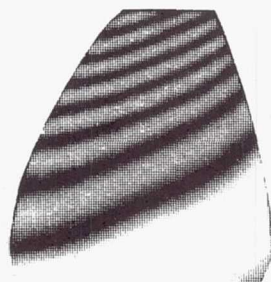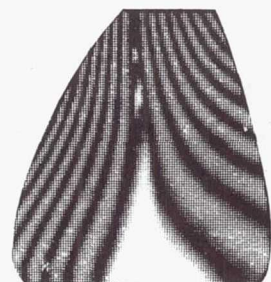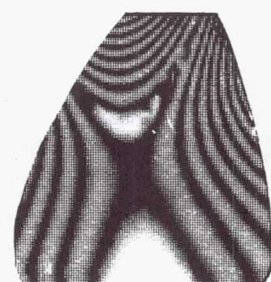
| 1020.4 Hz | 1752.6 Hz | 2525.2 Hz | 3326.7 Hz |
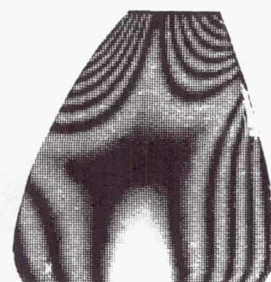
Figure 18. — Results for CM2 forward blade.

Experimental			
953 Hz	1768 Hz	2319 Hz	2959 Hz

NASTRAN			
963.2 Hz	1939.7 Hz	2518.7 Hz	3252.9 Hz

MARC			
1033.6 Hz	1837.1 Hz	2507.8 Hz	3158.8 Hz

Figure 19. — Results for CM2 aft blade.

Conclusions

For the shell elements used in this study, displacement-dependent centrifugal forces are accounted for by MARC in the dynamic analysis of rotating, flexible structures. Unlike NASTRAN (ref. 6), MARC does not require special programming to account for these forces. However, when springs are coupled to a MARC finite element model subjected to centrifugal loading, a simple test, such as the rotating spring-mass problem, should be made on the chosen finite element to ensure inclusion of centrifugal-softening terms in the stiffness matrix.
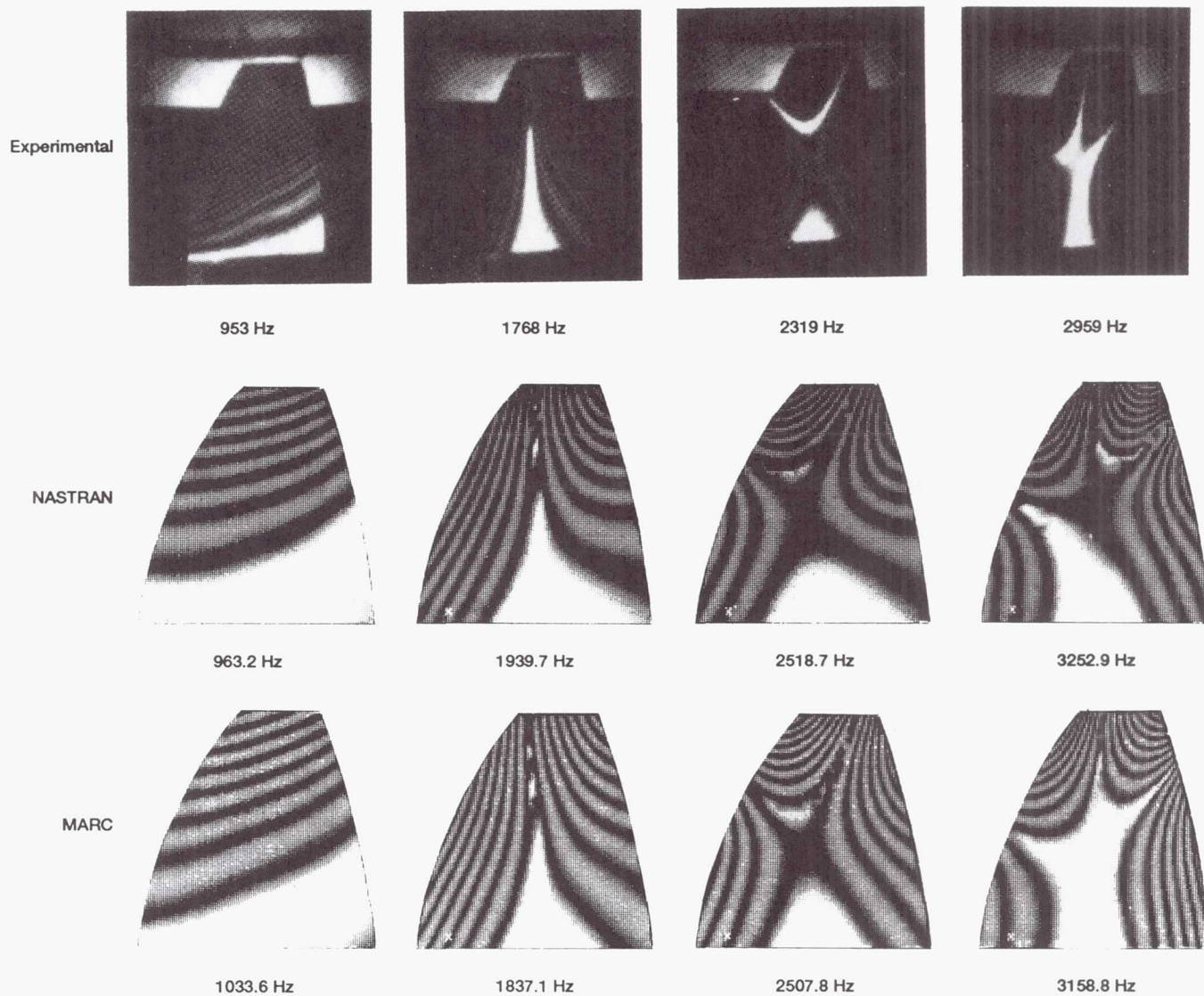
The isotropic twisted plate study and the analyses conducted on the composite propfan blades show that MARC's quadrilateral elements 75 and 22 are capable of handling the complex geometric attributes of blades (i.e., twist and curvature). The use of equivalent orthotropic material properties of composite laminates is suitable when generating MARC models of composite blades with COBSTRAN. However, these material properties must be defined about the material axis of symmetry. A recurrent composite ply pattern is recommended for use in the design of the propfan blade.

Keeping in mind the aforementioned limitations, the use of MARC coupled with COBSTRAN offers the analyst an alternate approach for analyzing rotating composite blades. The COBSTRAN-MARC methodology can be used in place of, or in conjunction with, the current COBSTRAN-NASTRAN approach. This methodology provides the analyst with greater versatility because of MARC's extensive nonlinear capabilities.
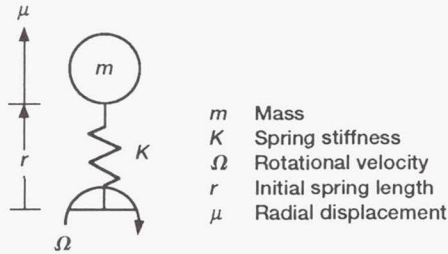
Lewis Research Center
National Aeronautics and Space Administration
Cleveland, Ohio, July 21, 1992

References

1. Hager, R.D.; Vrabel, D.V.: Advanced Turboprop Project. NASA SP–495, 1988.
2. Aiello, R.A.; and Chamis, C.C.: Composite Blade Structural Analyzer (COBSTRAN) Theoretical/Programmer's Manual. NASA TM–101958, 1989.
3. Fong, H.H.: MARC Primer. MARC Analysis Research Corp., Palo Alto, CA., 1989.
4. Leissa, A.; and Co, C.-M.: Coriolis Effects on the Vibrations of Rotating Beams and Plates. Proceedings of the Twelfth Southeastern Conference on Theoretical and Applied Mechanics, Vol. 2, Auburn University Press, Montogomery AL, 1984, pp. 508–513.
5. Subrahmanyam, K.P.; and Kaza, K.R.V.: Vibration and Buckling of Rotating, Pretwisted, Preconed Beams Including Coriolis Effects. J. Vib., Acous., Stress Reliab. Des., vol. 108, no. 2, Apr. 1986, pp. 140–149.
6. Lawrence, C., et al.: A NASTRAN Primer for the Analysis of Rotating Flexible Blades. NASA TM–89861, 1987.
7. User Information Manual. Vol. A, Rev. K.4. MARC Analysis Research Corp., Palo Alto, CA, Jan. 1990.
8. Program Input. Vol. C, Rev. K.4. MARC Analysis Research Corp., Palo Alto, CA, Jan. 1990.
9. MARC Element Library. Vol. B, Rev. K.4. MARC Analysis Research Corp., Palo Alto, CA, Jan. 1990.
10. Ernst, M.A.; and Lawrence, C.: Hub Flexibility Effects on Propfan Vibration. NASA TM–89900, 1987.
11. Kielb, R.E.; Liessa, A.W.; and MacBain, T.C.: Vibrations of Twisted Cantilever Plates – A Comparison of Theoretical Results. Int. J. Numer. Methods Eng., vol. 21, no. 8, Aug. 1985, pp. 1365–1380.
12. Kielb, R.E., et al.: Joint Research Effort on Vibrations of Twisted Plates. NASA RP–1150, 1985.
13. MacBain, J.C.; et al.: Vibrations of Twisted Cantilever Plates – Experimental Investigation. ASME Paper 84–GT–96, 1984.
14. Aiello, R.A.: Composite Blade Structural Analyzer (COBSTRAN) User's Manual. NASA TM–101461, 1989.
15. Stefko, G.L., et al.: Overview of Cruise Missile Composite Propfan Design, Analysis and Fabrication. NASA TM–105264, 1992.
16. Miller, C.J.: Aerodynamic Design of Aft-Mounted Counter Rotating Propfans for a Cruise Missile Model. NASA TM–105265, 1992.
17. Thorp, S.A.; Downey, K.M.: Computer Aided Design and Manufacturing of Composite Propfan Blades for a Cruise Missile Wind Tunnel Model. NASA TM–105269, 1992.
18. Ernst, M.A.: Structural Analysis of Low RPM Composite Propfan Blades for the LRCSW Wind Tunnel Model. NASA TM–105266, 1992.
19. Carek, D.A.: Structural Analysis of High RPM Composite Propfan Blades for a Cruise Missile Wind Tunnel Model. NASA TM–105267, 1992.
20. Miller, C.J.: Holographic Testing of Composite Propfans for a Cruise Missile Wind Tunnel Model. NASA TM–105271, 1992.
21. Fite, E.B.: Fabrication of Composite Propfans for a Cruise Missile Wind Tunnel Model. NASA TM–105270, 1992.

Appendix A
Equation of Motion for a Rotating Spring-Mass System

m	Mass
K	Spring stiffness
Ω	Rotational velocity
r	Initial spring length
μ	Radial displacement

The moment of inertia I about the rotational axis is written as

$$I = m(r+\mu)^2$$

The kinetic energy κ is written as

$$\kappa = 1/2\,I\Omega^2 + 1/2\,m\,\dot{\mu}^2$$

$$= 1/2\,m(r+\mu)^2\,\Omega^2 + 1/2\,m\,\dot{\mu}^2$$

The potential energy V is written as

$$V = 1/2\,K\mu^2$$

The Lagrangian L is then

$$L = \kappa - V$$
$$= 1/2\,m(r+\mu)^2\Omega^2 + 1/2\,m\,\dot{\mu}^2 - 1/2\,K\mu^2$$

Applying Lagrange's equation

$$\frac{\partial L}{\partial \mu} - \frac{d}{dt}\left(\frac{\partial L}{\partial \dot{\mu}}\right) = 0$$

the equation of motion is derived as

$$m(r+\mu)\Omega^2 - K\mu - m\ddot{\mu} = 0$$

$$m\ddot{\mu} + K\mu = m\Omega(r+\mu)$$

$$m\ddot{\mu} + [K - \underbrace{m\Omega^2}]\mu = m\Omega^2 r$$

centrifugal−softening term

Appendix B
Summary of MARC Shell Element Formulations

Element 3	Quadrilateral or triangular 4-node 2 degrees of freedom Isoparametric Plane stress Uniform thickness at nodes	Element 26	Quadrilateral or triangular 8-node 2 degrees of freedom Isoparametric Plane stress Uniform thickness at nodes
Element 22	Quadrilateral or triangular 8-node 6 degrees of freedom Transverse shear effects Variable thickness at nodes	Element 75	Quadrilateral or triangular 4-node 6 degrees of freedom Transverse shear effects Variable thickness at nodes

REPORT DOCUMENTATION PAGE

Public reporting burden for this collection of information is estimated to average 1 hour per response, including the time for reviewing instructions, searching existing data sources, gathering and maintaining the data needed, and completing and reviewing the collection of information. Send comments regarding this burden estimate or any other aspect of this collection of information, including suggestions for reducing this burden, to Washington Headquarters Services, Directorate for Information Operations and Reports, 1215 Jefferson Davis Highway, Suite 1204, Arlington, VA 22202-4302, and to the Office of Management and Budget, Paperwork Reduction Project (0704-0188), Washington, DC 20503.

1. AGENCY USE ONLY (Leave blank)	2. REPORT DATE	3. REPORT TYPE AND DATES COVERED
	March 1993	Technical Memorandum

4. TITLE AND SUBTITLE	5. FUNDING NUMBERS
Evaluation of MARC for the Analysis of Rotating Composite Blades	WU 535-03-10
6. AUTHOR(S) Karen F. Bartos and Michael A. Ernst	

7. PERFORMING ORGANIZATION NAME(S) AND ADDRESS(ES)	8. PERFORMING ORGANIZATION REPORT NUMBER
National Aeronautics and Space Administration Lewis Research Center Cleveland, Ohio 44135-3191	E-7163

9. SPONSORING/MONITORING AGENCY NAMES(S) AND ADDRESS(ES)	10. SPONSORING/MONITORING AGENCY REPORT NUMBER
National Aeronautics and Space Administration Washington, D.C. 20546-0001	NASA TM-4423

11. SUPPLEMENTARY NOTES

Responsible person, Karen F. Bartos, (216) 433-6478.

12a. DISTRIBUTION/AVAILABILITY STATEMENT	12b. DISTRIBUTION CODE
Unclassified - Unlimited Subject Category 39	

13. ABSTRACT (Maximum 200 words)

The suitability of the MARC code for the analysis of rotating composite blades was evaluated using a four-task process. A nonlinear displacement analysis and subsequent eigenvalue analysis were performed on a rotating spring-mass system to ensure that displacement-dependent centrifugal forces were accounted for in the eigenvalue analysis. Normal modes analyses were conducted on isotropic plates with various degrees of twist to evaluate MARC's ability to handle blade twist. Normal modes analyses were conducted on flat composite plates to validate the newly developed coupled COBSTRAN-MARC methodology. Finally, normal modes analyses were conducted on four composite propfan blades that were designed, analyzed, and fabricated at NASA Lewis Research Center. Results were compared with experimental data. The research documented herein presents MARC as a viable tool for the analysis of rotating composite blades.

14. SUBJECT TERMS		15. NUMBER OF PAGES
Propfan technology; MARC; Composites; Finite element method		28
		16. PRICE CODE A03

17. SECURITY CLASSIFICATION OF REPORT	18. SECURITY CLASSIFICATION OF THIS PAGE	19. SECURITY CLASSIFICATION OF ABSTRACT	20. LIMITATION OF ABSTRACT
Unclassified	Unclassified	Unclassified	

NSN 7540-01-280-5500